Supplementary Data

Structure of the cytosolic G protein alpha chaperone and guanine nucleotide exchange factor Ric-8A bound to Gαi1

McClelland, *et al.*

Supplementary Table 1
Cryo-EM Data Collection and Refinement Statistics

Data collection and processing	Ric-8A(491):Δ31NGαi1:4Nb
Microscope	Titan Krios
Voltage (kV)	300
Camera	Gatan K2 Summit
Pixel size (Å)	1.06
Total Dose (e-/Å^2)	69
Defocus range (μm)	-1 to -3
Number of micrographs	8,670
Number of initial particles	768,736
Symmetry	C1
Number of final particles	327,493
Resolution (0.143 FSC, Å)	3.90
Atomic model refinement	
Software	phenix.real_space_refine
Clashscore, all atoms	8.79
Poor rotamers (%)	0.57
Favored rotamers (%)	99.43
Ramachandran favored (%)	84.24
Ramachandran allowed (%)	15.76
MolProbity score	2.15
Bond RMSD (Å)	0.006
Angle RMSD (Å)	1.005

Supplementary Table 2
Crystallographic Data Collection and Refinement Statistics

Data collection	Ric-8A(491):Δ31NGαi1:3NB		
Software	AutoPROC/STARANISO	XDS/AIMLESS	SCALA
Reflection scaling method[#]	Anisotropic filtered (extended)	Isotropic (extended)	Isotropic (standard)
Wavelength (Å)	0.979	0.979	0.979
Resolution range (Å)*	39.58 - 3.3 (3.9 - 3.3) [a*, b*=4.6, c*=3.3]	39.65 - 3.3 (3.9 - 3.3)	39.65 - 4.6 (4.7 - 4.6)
Space group	P 2_1	P 2_1	P 2_1
Unit cell dimensions			
a, b, c (Å)	93.0 144.7 114.4	93.0 144.7 114.4	93.0 144.7 114.4
β (^{o})	94.7	94.7	94.7
Total reflections*	73843 (3449)	160159 (62218)	58730 (2930)
Unique reflections*	20707 (1035)	44840 (17203)	16296 (796)
Redundancy*	3.6 (3.3)	3.6 (3.6)	3.6 (3.7)
Completeness [spherical] (%)*	45.8 (6.0)	99.1 (99.1)	99.1 (99.5)
Completeness [ellipsoidal] (%)*	90.1 (58.2)	98.3 (91.5)	
Mean I/σ (I)*	3.7 (1.7)	1.9 (0.3)	4.1 (2.2)
Wilson B-factor	91.88		
R_{meas} [†,*]	0.21 (0.70)	0.55 (4.65)	0.18 (0.54)
$R_{p.i.m.}$ [†,*]	0.11 (0.38)	0.29 (2.42)	0.10 (0.28)
$CC_{1/2}$ [†]	0.99 (0.70)	0.97 (0.17)	0.99 (0.86)
Refinement			
R_{work} [†,*]	0.248 (0.319)		
R_{free} [†,*]	0.287 (0.323)		
CC_{work} [†*]	0.907 (0.719)		
CC_{free} [†*]	0.866 (0.893)		
Number of total atoms			
protein	15938		
total protein residues	2021		
RMS deviations			
bond lengths (Å)	0.002		
bond angles (◦)	0.55		
Ramachandran favored (%)[††]	89.16		
Ramachandran allowed (%)[††]	10.53		
Ramachandran outliers (%)[††]	0.30		
Rotomer outliers (%)[††]	0.0		
Clash Score[††]	10.32		
Average B-factor			
Macromolecules	109.97		
Number of TLS groups	1		

[#] The standard isotropic scaling method uses the classical isotropic treatment in truncate program where the resolution cut is determined by (1) Rpim ≤ 0.6. average I/σ(I) in a resolution bin ≥ 2.0, and $CC_{1/2}$ ≥ 0.3. The extended isotropic method includes all the measurements within the sphere of the highest observed resolution limit where the local [I/σ(I) ≥ 1.2; the extended anisotropic method uses the anisotropically-filtered reflections by STARANISO with the same resolution limit as the extended isotropic method. [*] Data for highest resolution shell are given in brackets. [†] $R_{meas}=\sum_{hkl}(n/n\text{-}1)^{1/2}\sum_i |I_i(hkl)-\langle I(hkl)\rangle|/\sum_{hkl}\sum_i I_i(hkl)$, where $I_i(hkl)$ is the ith observation of the intensity of the reflection hkl and $\langle I_{hkl}\rangle$ is the mean over n observations. $R_{p.i.m.}=\sum_{hkl}(1/n\text{-}1)^{1/2}\sum_i |I_i(hkl)-\langle I(hkl)\rangle|/\sum_{hkl}\sum_i I_i(hkl)$. [§] $R_{work}=\sum_{hkl}||F_{obs}|-|F_{calc}||/\sum_{hkl}|F_{obs}|$, where F_{obs} and F_{calc} are the observed and calculated structure-factor amplitudes for each reflection hkl. R_{free} was calculated for 5% of the diffraction data that were selected randomly and excluded from refinement. Correlation coefficients: $CC = \Sigma_i((x_i - \langle x\rangle)(y_i - \langle y\rangle))/(\Sigma_i((x_i - \langle x\rangle)^2(y_i - \langle y\rangle)^2)^{1/2}$, where x_i and y_i are the ith of n observations of quantities whose mean values are $\langle x\rangle$ and $\langle y\rangle$; for $CC_{1/2}$, x_i, and y_i correspond to intensity measurements derived from each of two randomly selected half-data sets from the set of unmerged data; For CC_{work} and CC_{free} x_i and y_i refer to observed structure factor amplitudes and structure factor amplitudes computed from the refined atomic model, respectively, for the working data set and the set used to compute R_{free}. [††]Calculated using MolProbity

a

```
NB_8109 AQVQLQESGGGLEQAGDSLRLSCAASGLIVSNYAMGWFRQAPGKEREFVAYINWNGGVTY 60
NB_9156 -QVQLQESGGGLEQAGDSLRLSCAASGLIVSNYAMGWFRQAPGKEREFVAYINWNGGVTY 59
NB_8117 -QVQLQESGGGLVQPGGSLRLSCAASGIIFRSNGMAWYRQAPGKEREWVASITSFGDA-I 58
NB_8119 -QVQLQESGGGLVQAGGSLRLSCAASGGIVHISSMGWFRQAPGKQRELVATSPSNGDI-R 58
         *********** * *.********** *.   .*.*:******:** **     *.

NB_8109 YTNSVKGRFTISRDNAKNTVYLQMNSLKPEDTAVYYCARTSRASVTTRVADFGYWGQGTQ 120
NB_9156 YTNSVKGRFTISRDNAKNTVYLQMNSLKPEDTAVYYCARTSRASVTTRVADFGYWGQGTQ 119
NB_8117 YRDSVKGRFTISRDNARNAVSLQTNSLKTEDTAVYYCNTYPV---------NSAWGQGTQ 109
NB_8119 YADSVKGRFTLSRDNAKNTVSLQMNSLEPEDTAVYYCHSFLRHTAS--ASYNNYYGQGTQ 116
        * :*******:*****:*:* ** ***: ********              . :*****

NB_8109 VTVSSHHHHHHEPEA 135
NB_9156 VTVSSHHHHHHEPEA 134
NB_8117 VTVSSHHHHHHEPEA 124
NB_8119 VTVSSHHHHHHEPEA 131
        ***************
```

b

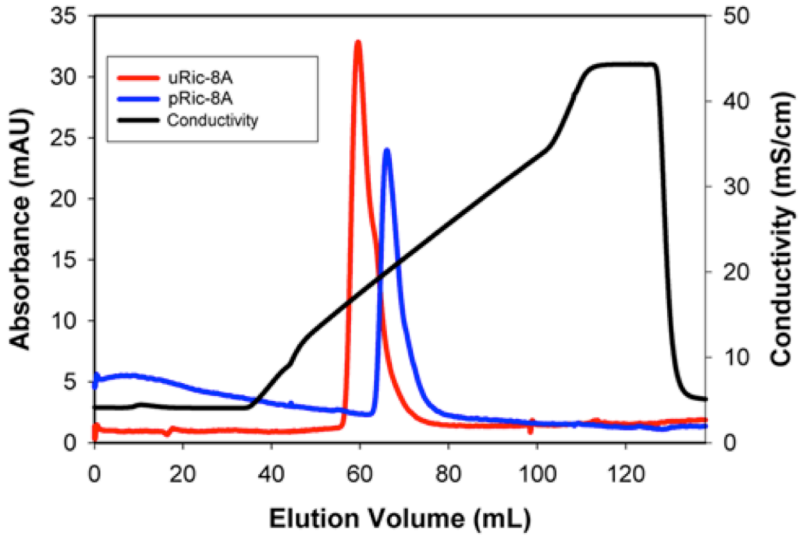

c

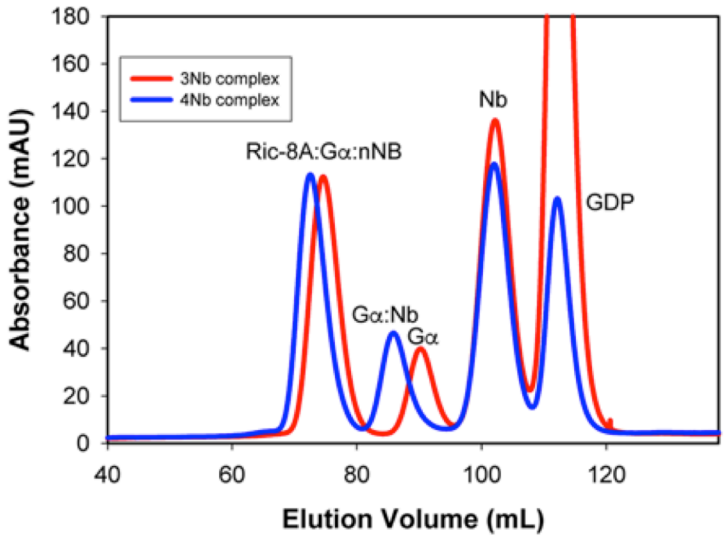

Supplementary Figure 1. Purification of Ric-8A:Gα:Nb complexes. **a**, Amino acid sequences of nanobodies used to form complexes. **b**, Anion exchange chromatography of phosphorylated (pRic-8A) and unphosphorylated (uRic-8A). **c**, Gel filtration of complexes at the following molar stoichiometric ratios: 1 Ric-8A:2 Gα:2 Nb 8109:2 Nb 8117:2 Nb 8119 (*red)* and 1 Ric-8A:2 Gα:2 Nb 8109:2 Nb 8117:2 Nb 8119:4 Nb 9156 (*blue*) molar stoichiometric ratios, Ric-8A and Gα correspond to the 1-491 residue construct of Ric-8A and the 31N-terminal truncation mutant of Gαi1, respectively, as described in the main text. (see Methods).

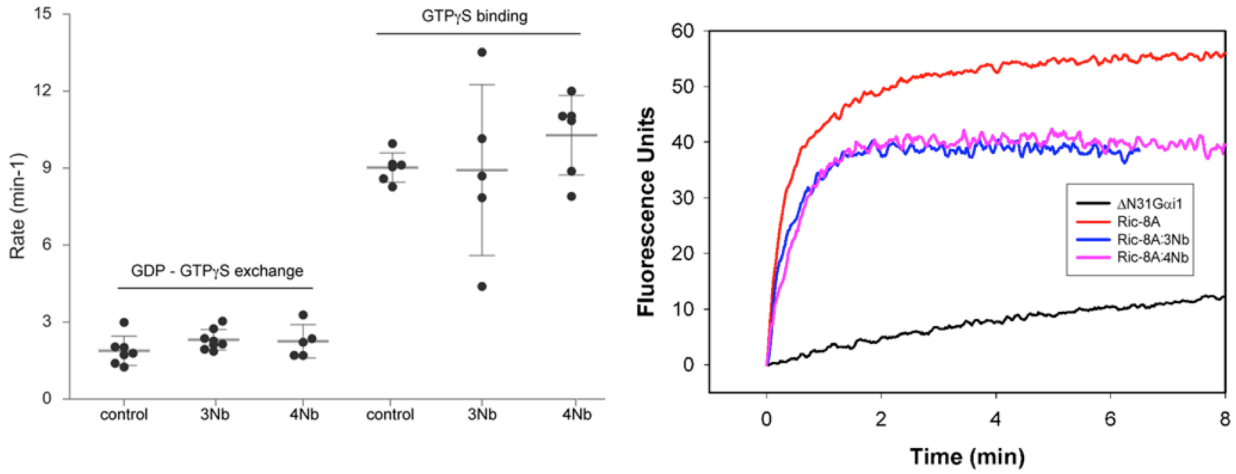

Supplementary Figure 2 Effect of nanobodies on GEF activity of Ric-8A. a, GDP-GTP exchange rates were measured by the rate of tryptophan fluorescence increase upon addition of ΔN31Gαi1 to Ric-8A and GTPγS at final concentrations of 2μM Ric-8A, 1μM ΔN31Gαi1 and 10μM GTPγS in the absence (control) or presence of Nb 8109 (4 μM), Nb 8117 (4 μM), Nb 8119 (4 μM) (3Nb) or the latter with the addition of (4 μM) Nb 9156 (4Nb). GTP binding rates were measured by tryptophan fluorescence increase upon addition of GTPγS (10 μM final concentration) to size exclusion chromatography-purified Ric-8A:ΔN31Gαi1:nNb (1 μM). Progress curves for the 3Nb and 4Nb GDP-GTPγS exchange and 4Nb GTPγS binding assays were fit to a single exponential rate, whereas data for controls and the 3Nb GTPγS binding assay were fit to a double exponential model, due to the presence of a slow kinetic phase, and the kinetic constant of the fast rate (k1) reported. In all cases average and standard deviations of measurement are reported for a minimum of 5 experimental replicates. **b**, Sample progress curves for the data reported in panel **a.**

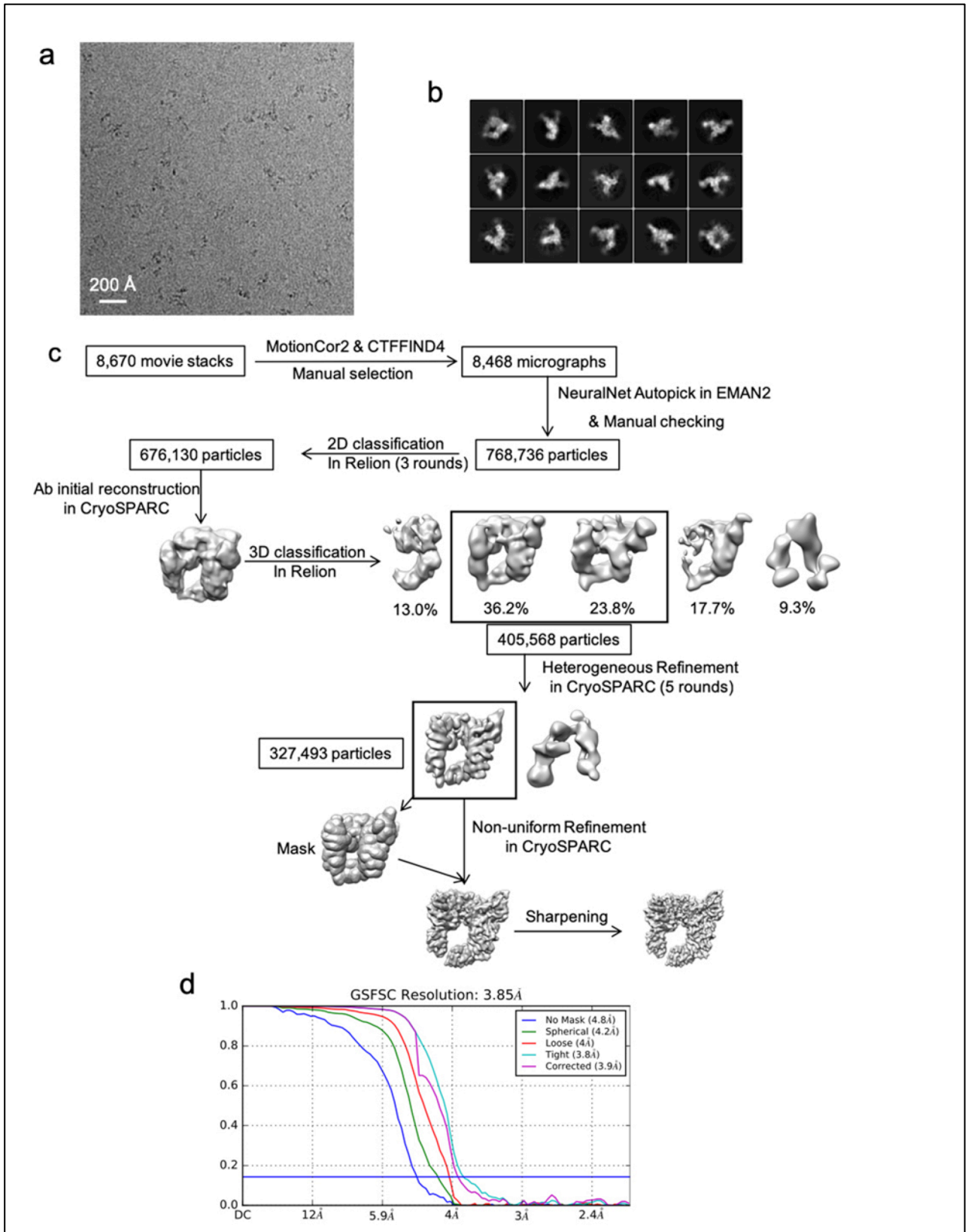

Supplementary Figure 3. Single-particle cryo-EM of Ric-8A:Gα:4Nb complex and Workflow of cryo-EM image processing. a, Representative motion corrected cryo-EM micrograph. **b**, Reference-free 2D Class averages computed in Relion. **c**, Workflow for cryo-EM processing (see Methods). **d**, Gold-standard Fourier Shell Correlation plot for 3D reconstruction generated using CryoSPARC.

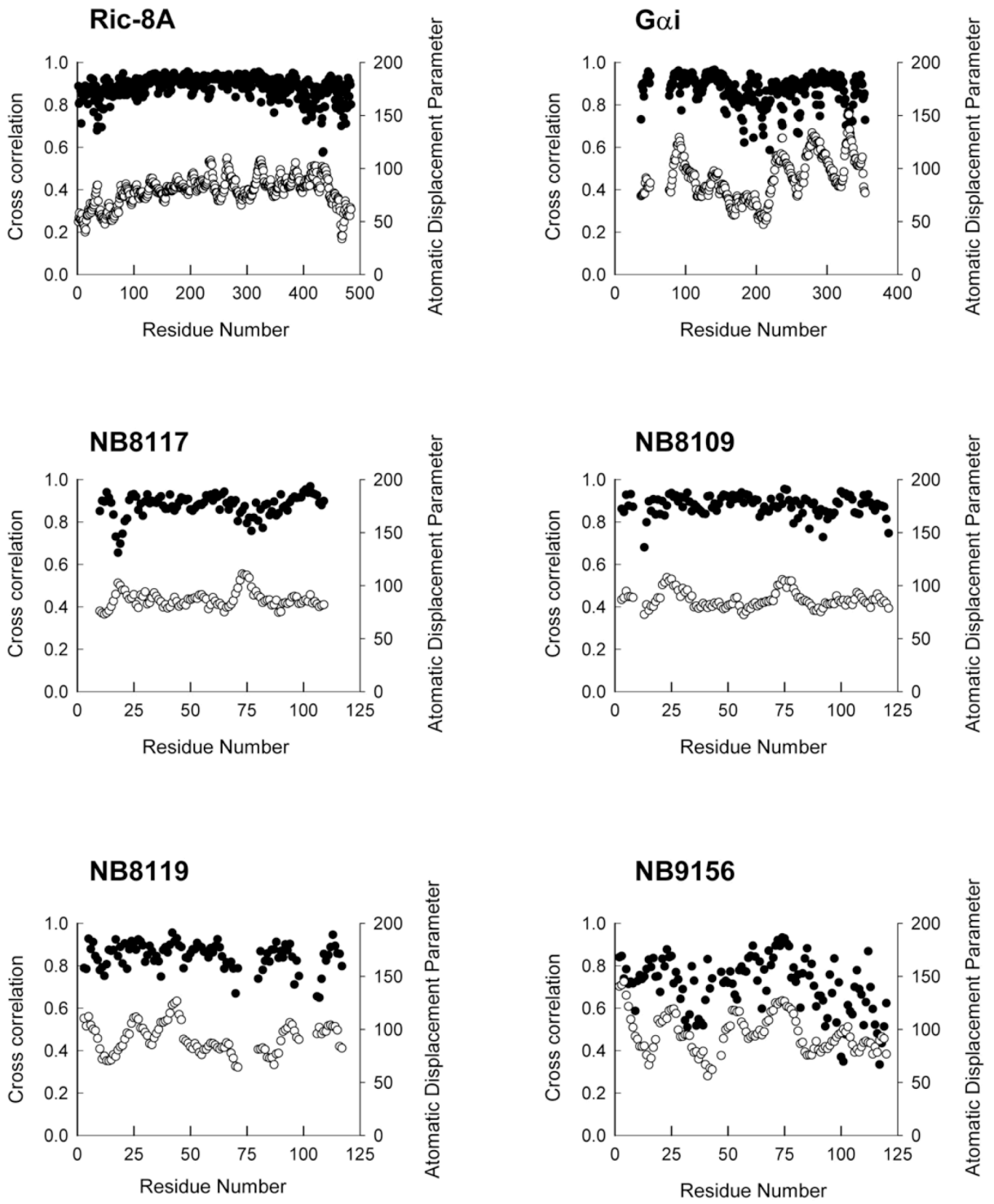

Supplementary Figure 4. Real-space refinement of Ric-8A:Gα model fit to cryo-EM map. Model-map correlation (filled circles) and atomic displacement parameter (open circles) are plotted with respect to residue number for the macromolecular components of the Ric-8A:Gα:4NB model derived from cryo-EM map. Data were generated using the phenix.real space refine program from the PHENIX suite.

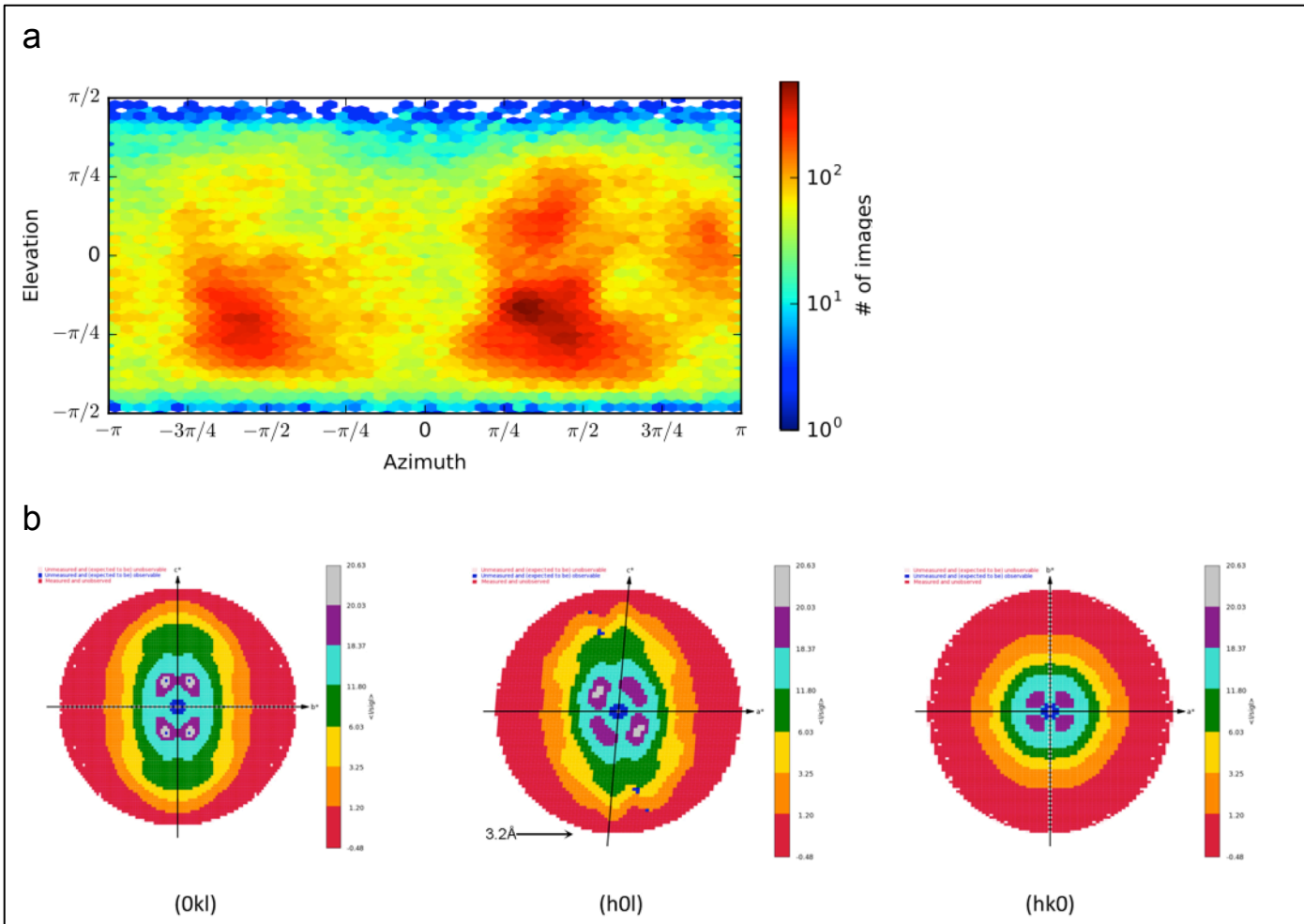

Supplementary Figure 5 Completeness of Cryo-EM and X-ray crystallographic data in real and reciprocal space. a, Distribution of particle orientations, generated using cryoSPARC in images used to generate 3D cryo-EM reconstruction. **b,** Projections of diffraction intensities from crystals of the Ric-8A:Gα:3Nb complex along reciprocal cell axes and color-coded by I/σI. Data generated using the STARANISO sever (see Methods).

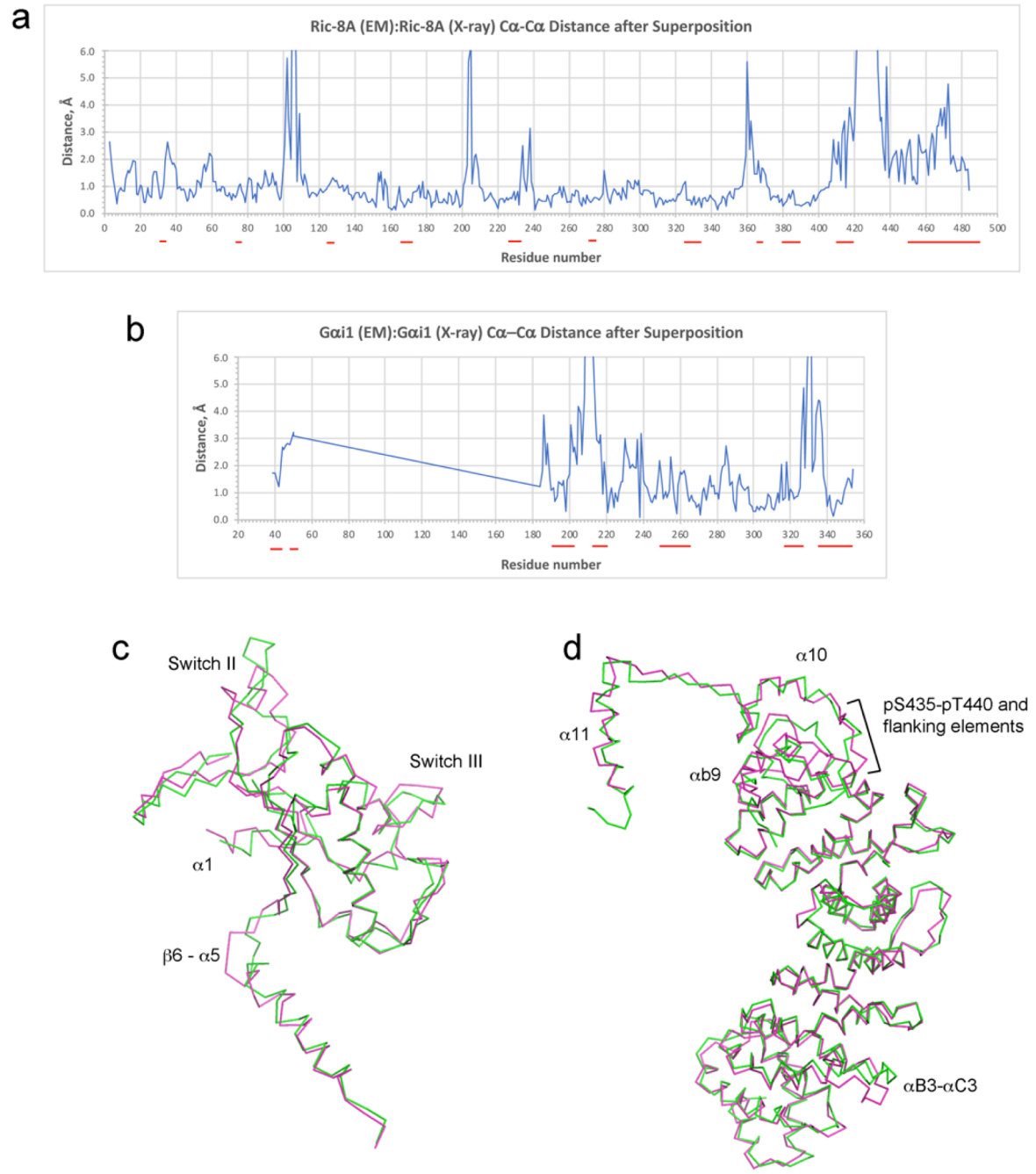

Supplementary Figure 6. Agreement of cryo-EM and X-ray structures of Ric-8A:Gαi1. a, Deviation between corresponding Cα atoms after least-squares superposition of Ric-8A coordinates. *Red* lines below residue numbers mark regions at which Ric-8A contacts Gai1 (see also ED Figure 10). The RMSD for all 484 common Cα positions is 1.81Å. The PyMOL align routine yields an RMSD of 1.03Å after rejection of 69 outliers. **b**, Deviation between Gαi1 atoms, computed per panel **a**. The RMSD for all 183 common Cα positions is 2.36Å; PyMol align yields an RMSD of 1.49Å after rejection of 21 outliers**. c,** Superposition of cryoEM (*magenta*) and X-ray (*green*) structures of Gαi1. Structural elements that show the largest structural differences are labeled. **d**, Superposition of Ric-8A models, as per panel **c.**

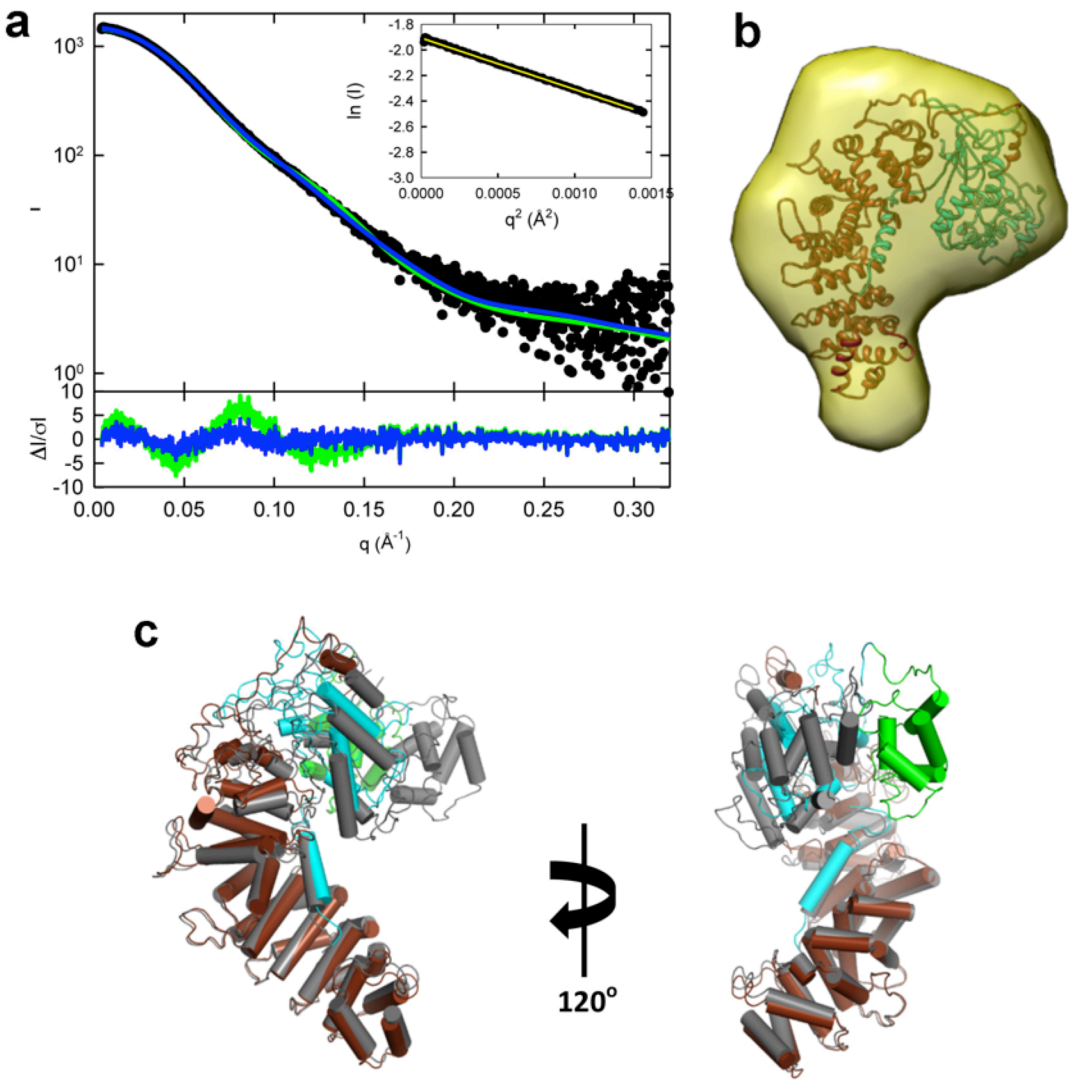

Supplementary Figure 7. Solution structure and Normal Mode refined model of Ric-8A:Δ31NGαi1 complex from Small-Angle X-ray scattering. **a**, Solution scattering profile for Ric-8A:ΔN31Gαi1 complex (*closed circles*). Inset shows, associate Guinier plot. CRYSOL and SRELEX from the ATSAS software package were used, respectively, to compute scattering profiles from atomic coordinates, and use normal-mode analysis to generate a refined atomic model. Computed scattering curves for cryo-EM-derived atomic coordinates of Ric-8A:ΔN31Gαi1 complex are shown in *green* and that from normal mode analysis is rendered in *blue*. The χ^2 for the fit of the computed scattering curve for the cryo-EM model is 5.48 and that for the normal-mode refined model is 1.24. The bottom panel shows the error-weighted residual difference plots $\Delta I/\sigma I = (I(q)_{experimental} - CI(q)_{model})/\sigma I(q)$ *vs* q, where C is a normalizing scale factor. **b,** SREFLEX-refined Ric-8A:ΔN31Gαi1 model fit to the *ab initio* molecular envelope calculated from the experimental SAXS scattering curve (*yellow*). **c**, Superposition of the SREFLEX-refined model of Ric-8A:ΔN31Gαi (Ric-8A, *brown*; GTPase domain of ΔN31GαI, *cyan*; Helical domain of ΔN31GαI, *green*) onto the cryo-EM model (*gray*), indicating a mode of helical domain rotation that may be preferred in solution in the absence of nanobodies. Models were superimposed using the Cα atomic positions of Ric-8A.

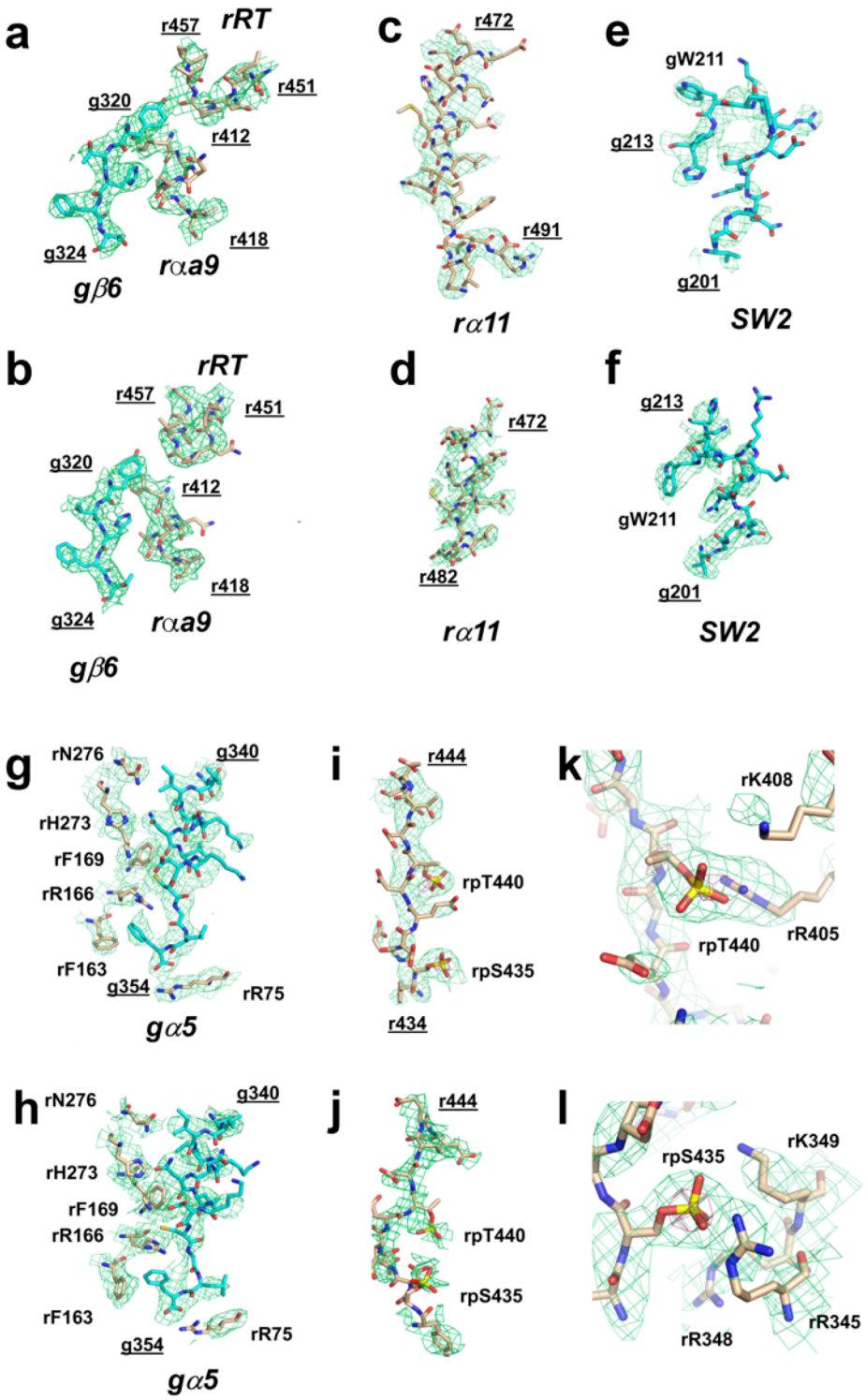

Supplementary Figure 8. X-ray and cryo-EM density at selected residue ranges. 2DFo-mFc electron density is contoured at 1.0σ and cryo-electron density is contoured at a threshold of 3.5. Structural elements of Ric-8A and Gαi1 are labeled in bold italics, N- and C-terminal residue numbers of segments are shown underlined, selected residues are labeled. Carbon atoms in Ric-8A are colored *wheat* and in Gαi1, *cyan*. Panels **a, c, e, g** and **i** show residues from crystallographic model with corresponding density. Panels **b, d, f, h** and **j** show the same from the cryo-EM model. Panels **k** and **l**, show the crystallographic model and associated density around phospho-serine 435 and phospho-threonine 440, respectively. The 5σ contour level is shown in *red*.

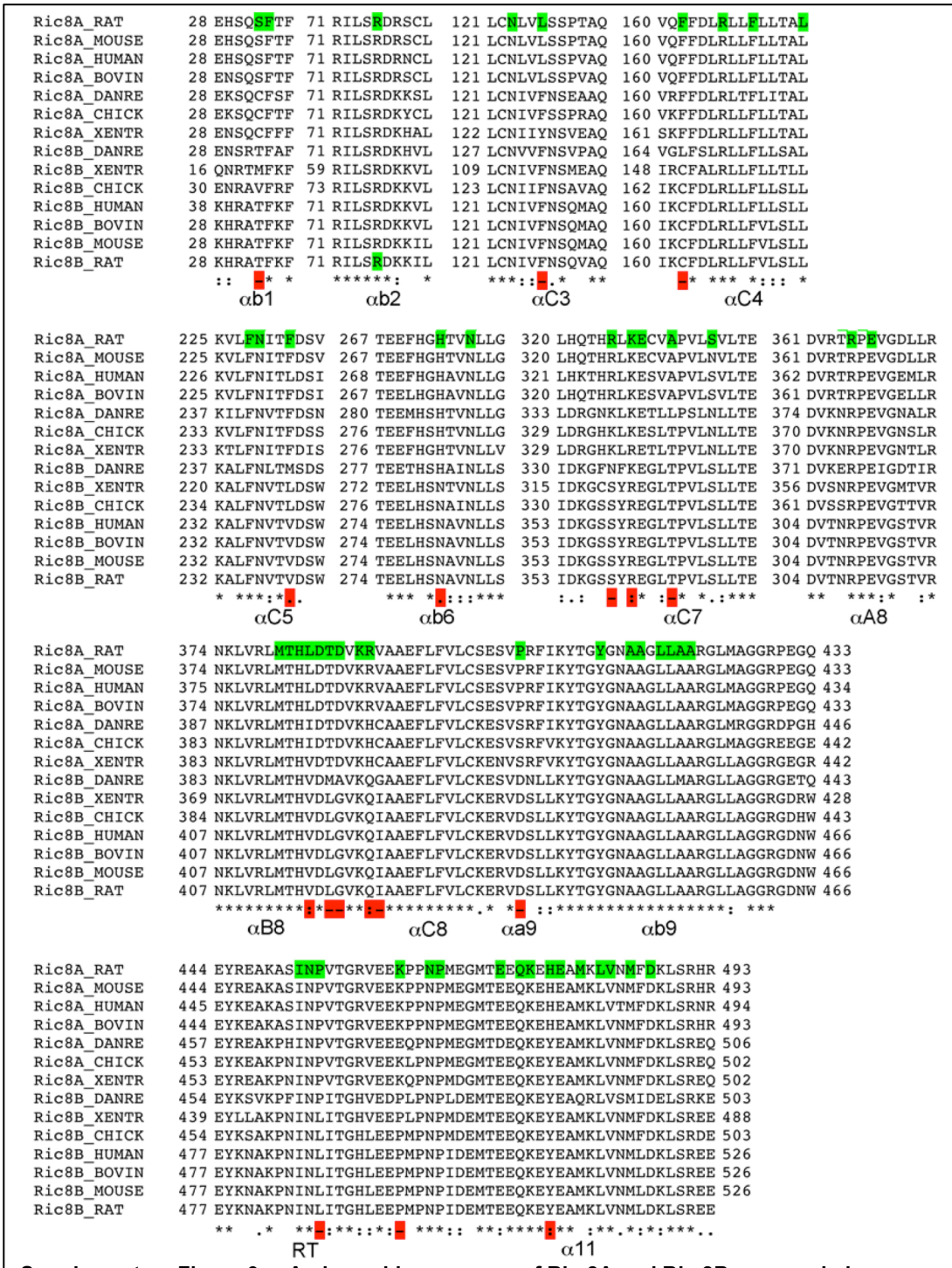

Supplementary Figure 9a. Amino acid sequences of Ric-8A and Ric-8B across phylogeny near Gα contact residues. Residue numbers are shown at the start and, for long tracts, the end of subsequences that harbor Ric-8A contacting-residues, highlighted in *green* in the sequence of rat Ric-8A, defined as those that include at least one atom within 4.0 of an atom in Gαi1. Amino acids not identical in rat Ric-8A and rat Ric-8B in *red* in the conservation summary at the bottom of each alignment. Central residues of secondary structural elements are shown below the conservation summary.

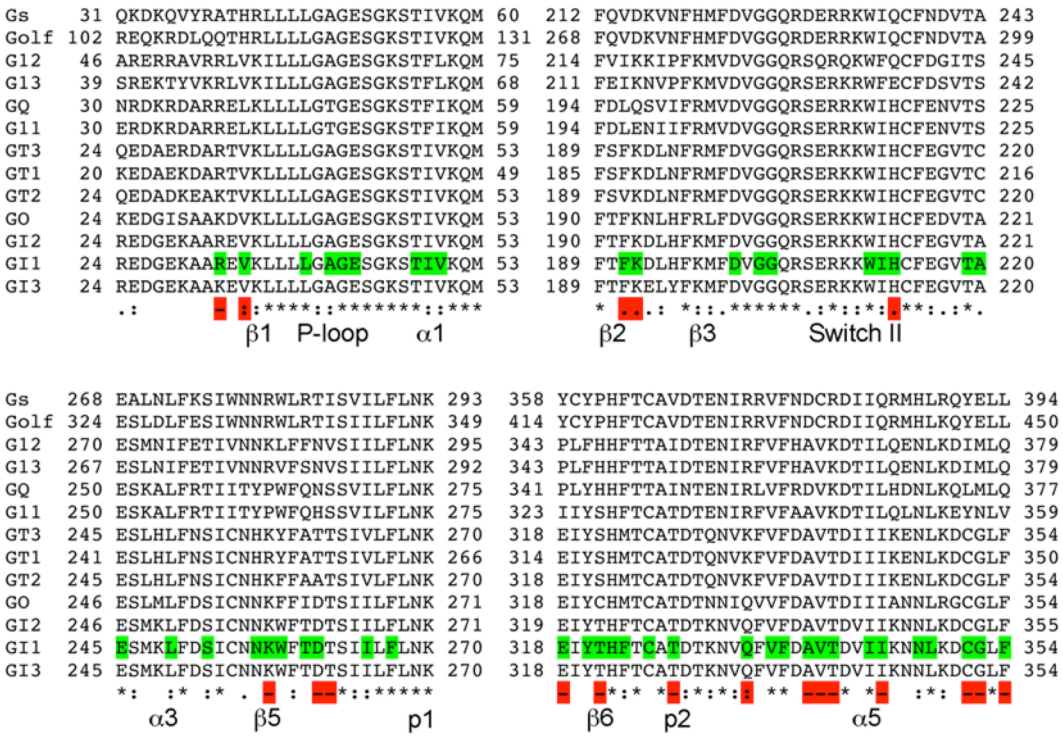

Supplementary Figure 9b. Sequence of rat Gα isoforms within Ric-8A contact regions. Residue numbers are shown at the start and end of subsequences that harbor Ric-8A contacting-residues, highlighted in *green* in the sequence of Gαi1, defined as those that include at least one atom within 4.0 of an atom in Ric-8A. Amino acids not identical in Gαi and Gαs are highlighted in *red*, in the conservation summary at the bottom of each alignment. Central residues of secondary structural elements are shown below the conservation summary. Symbols p1 and p2 denote guanine nucleotide purine binding sites formed at the β5-αG and β6-α5 loops, respectively.

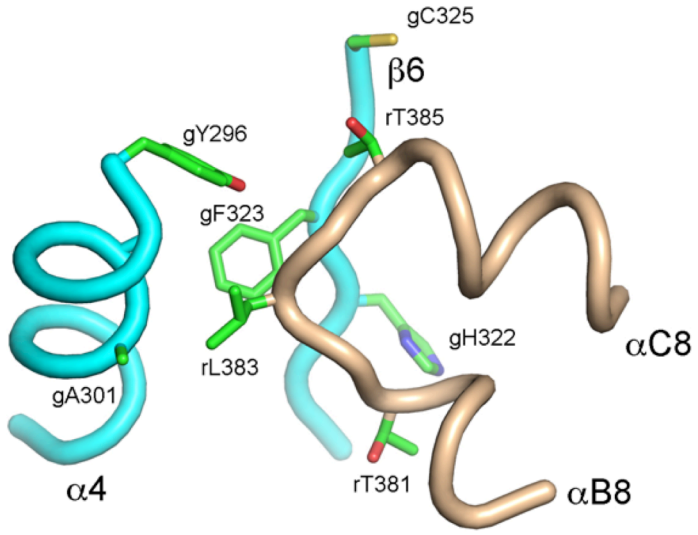

Supplementary Figure 10. Detail of Ric-8A:Gαi1 contact involving Gαi1 α4 and β6 with Ric-8A αB8-αC8. The crystal structure is shown with Gαi1 backbone in *cyan* and Ric-8A backbone in *wheat* with side-chain atom colors, carbon, *green*, nitrogen, *blue*, oxygen, *red* and sulfur, *yellow*. Mutation of rL383 to glutamate reduces GEF activity to 50% that of wild-type Ric-8A.

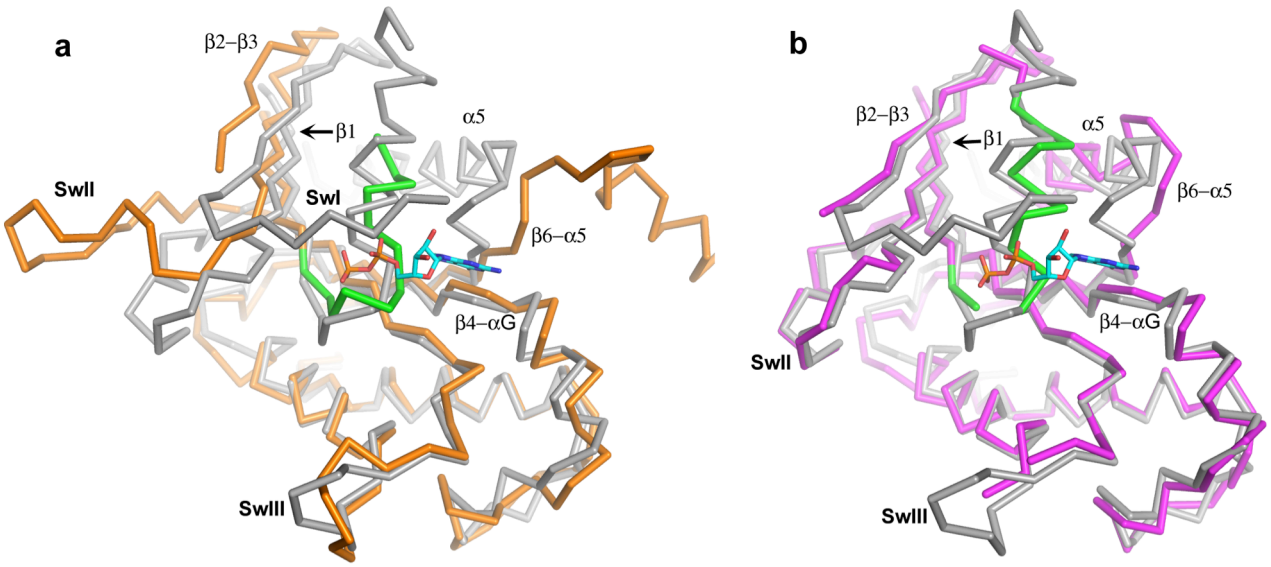

Supplementary Figure 11. Conformational perturbations induced in the Gα Ras domain by Ric-8A and a G protein-coupled Receptor. a, Cα-ribbon diagram showing superposition of Gαi1•GDP from the complex with Gβ1 and Gγ2 (PDB 1GG2), *gray*, onto the Ras domain of Gαi1, orange, bound to Ric-8A using residues 32-50 and 184-326. The α1 helix and P-loop of Ric-8A-bound Gαi1 is rendered *green*. GDP is shown as a stick model. **b**, Gαi1•GDP, as in panel **a** is shown superimposed, using the same residues, onto the Ras domain of Gαi2, magenta, bound to the A_1 Adenosine receptor (PDB 6D9H).